catalysts

MDPI

Article

The Impact of Pressure and Hydrocarbons on NO_x Abatement over Cu- and Fe-Zeolites at Pre-Turbocharger Position

Deniz Zengel [1], Simon Barth [1,2], Maria Casapu [1] and Jan-Dierk Grunwaldt [1,2,*]

[1] Institute for Chemical Technology and Polymer Chemistry (ITCP), Karlsruhe Institute of Technology (KIT), Engesserstr. 18/20, 76131 Karlsruhe, Germany; deniz.zengel@kit.edu (D.Z.); simon.barth@kit.edu (S.B.); maria.casapu@kit.edu (M.C.)

[2] Institute of Catalysis Research and Technology (IKFT), Karlsruhe Institute of Technology (KIT), Hermann-von-Helmholtz-Platz 1, 76344 Eggenstein-Leopoldshafen, Germany

* Correspondence: grunwaldt@kit.edu; Tel.: +49-721-608-42120

Abstract: Positioning the catalysts in front of the turbocharger has gained interest over recent years due to the earlier onset temperature and positive effect of elevated pressure. However, several challenges must be overcome, like presence of higher pollutant concentrations due to the absence or insufficient diesel oxidation catalyst volume at this location. In this context, our study reports a systematic investigation on the effect of pressure and various hydrocarbons during selective catalytic reduction (SCR) of NO_x with NH_3 over the zeolite-based catalysts Fe-ZSM-5 and Cu-SSZ-13. Using a high-pressure catalyst test bench, the catalytic activity of both zeolite catalysts was measured in the presence and absence of a variety of hydrocarbons under pressures and temperatures resembling the conditions upstream of the turbocharger. The results obtained showed that the hydrocarbons are incompletely converted over both catalysts, resulting in numerous byproducts. The emission of hydrogen cyanide seems to be particularly problematic. Although the increase in pressure was able to improve the oxidation of hydrocarbons and significantly reduce the formation of HCN, sufficiently low emissions could only be achieved at high temperatures. Regarding the NO_x conversion, a boost in activity was obtained by increasing the pressure compared to atmospheric reaction conditions, which compensated the negative effect of hydrocarbons on the SCR activity.

Keywords: pre-turbo; selective catalytic reduction; NO_x removal; zeolites; pressure; hydrocarbons

Citation: Zengel, D.; Barth, S.; Casapu, M.; Grunwaldt, J.-D. The Impact of Pressure and Hydrocarbons on NO_x Abatement over Cu- and Fe-Zeolites at Pre-Turbocharger Position. *Catalysts* **2021**, *11*, 336. https://doi.org/10.3390/catal11030336

Academic Editor: Wenpo Shan

Received: 6 February 2021
Accepted: 5 March 2021
Published: 6 March 2021

1. Introduction

Since exhaust emissions from internal combustion engines have a significant impact on the environment and our health, the related regulations have become more stringent in recent years [1]. Among different pollutants, nitrogen oxides (NO_x) not only cause photochemical smog and acid rain formation but are also irritating for the human respiratory tract [2–5]. The reduction of their emissions can only partially be achieved by engine management [6,7] and catalytic converters are nowadays inevitable components of the exhaust system. Particularly, the selective catalytic reduction (SCR) of NO_x with ammonia (NH_3) [8,9] using ion-exchanged zeolites or vanadium-based catalysts [8,10] is known as one of the most efficient catalytic methods. However, although sufficient NO_x conversion is attained under normal engine working conditions, significant emissions occur particularly during the engine start [11] or at low exhaust gas temperatures that are present due to more efficient engine management [12]. Hence, either more active catalytic materials or more favorable reaction conditions are necessary to comply with progressively stricter emission regulations. Since the development of new materials is time consuming and costly, improvement of reaction conditions would be a more appealing approach. In this regard, one of the most important parameters promoting the catalytic reaction is temperature and numerous solutions proposed over the years include a closer location of the catalytic system towards the engine [13]. For instance, a very promising increase in activity

was obtained by positioning the NH_3-SCR catalyst in front of the turbocharger [14–17]. In addition to temperatures of up to 180 °C higher at this location [18], the residence time is enhanced due to the higher pressure. These effects might enable a reduction of catalyst volume up to 40–70%, as shown in the case of diesel oxidations catalyst (DOC) and diesel particulate filter (DPF) applications [19,20]. However, at this location several challenges have to be faced. As shown in our previous study [14], the presence of short chain hydrocarbons (HC), like C_3H_6, or SO_2 tremendously affects the catalytic activity of a Cu-SSZ-13 SCR catalyst. In addition, the HC presence also leads to the formation of undesirable byproducts and might contribute to noticeable gas phase reactions [21,22]. Especially at higher pressures, the homogeneous conversion of hydrocarbons, NO and NH_3 is promoted and might considerably affect the NH_3-SCR activity, as recently reported for a V-based SCR catalyst [23]. Under real application conditions such effects are to be expected, considering that there is little space upstream of the turbocharger and a DOC component might be absent. Hence, higher concentrations of various hydrocarbons may reach the NH_3-SCR catalyst and influence its performance.

With this study, we have extended our previous investigations [11] on the emerging potential of pre-turbocharger catalyst location to unveil the influence of different hydrocarbon classes on the activity of some of the most representative ion-exchanged zeolite-based SCR catalysts that are Fe-ZSM-5 and Cu-SSZ-13. For this purpose short-chain, long-chain, and aromatic hydrocarbons (i.e., propylene, *n*-dodecane and *o*-xylene, respectively) were added to the NH_3-SCR gas mixture. Their conversion and impact on the NO_x removal activity as well as byproduct formation were systematically monitored at various temperatures and pressures.

2. Results and Discussion

The impact of higher pressure, as present at the pre-turbocharger catalyst location, was investigated at first for the catalytic oxidation of hydrocarbons involving only oxygen and water vapors (14% O_2, 4.5% H_2O in N_2) or the standard SCR gas mixture (350 ppm NO, 350 ppm NH_3, 14% O_2 and 4.5% H_2O in N_2 balance), which is reported in Sections 2.1 and 2.2, respectively. The information obtained on the hydrocarbon conversion profile and byproduct formation was used to understand the variations in NH_3-SCR activity under these complex reaction conditions, as discussed in Section 2.3.

2.1. Hydrocarbon Oxidation at Elevated Pressure in the Presence of Oxygen

Before studying the impact of elevated pressure on the oxidation of propylene (C_3H_6), *n*-dodecane ($C_{12}H_{26}$) and *o*-xylene (C_8H_{10}) in a standard SCR gas mixture, hydrocarbon oxidation tests were conducted at ambient pressure for Fe-ZSM-5 and Cu-SSZ-13 (details on the catalysts, cf. Sections 3.1 and 3.2) in an oxidative gas mixture (14% O_2, 4.5% H_2O in N_2, cf. Section 3.3) at a gas hourly space velocity (GHSV) of 100,000 h^{-1}. The aim was to obtain information on the catalyst oxidation activity and on the formation of byproducts that could affect the SCR reaction. As depicted in Figure 1a, at atmospheric pressure the conversion of propylene on Fe-ZSM-5 starts at 250 °C and increases continuously up to 55% at 550 °C. Propylene was oxidized to a large extent to CO and CO_2, reaching 83% CO_x selectivity at the highest investigated temperature (Figure S3). The proportion of CO_2 is lower than that of CO over the entire tested temperature range (Figure 2a). This observation is in line with previous literature, which reported CO as a main byproduct of propylene oxidation and oxidation of CO to CO_2 only above 400 °C [24]. The most important byproducts detected apart from CO and CO_2 are shown in Table 1 and consist of formaldehyde (HCHO), acetaldehyde (CH_3CHO) and ethylene (C_2H_4). Especially formaldehyde, which is known to be toxic and carcinogenic, was formed in large quantities and reached concentrations of up to 24 ppm at 500 °C.

The increase in pressure resulted in a positive effect on the Fe-ZSM-5 oxidation activity, which is mainly due to the longer residence time [14,25]. About 35% higher propylene conversion was measured at 450 °C and 5 bar as compared to the activity at

1 bar. Nonetheless, complete propylene oxidation could not be attained under the testing conditions used in this study (maximum 86% oxidation activity at 550 °C and 5 bar). In addition to the higher conversion, a more complete oxidation could be observed. However, with pressure enhancement propylene is preferentially oxidized towards CO (Figure 2a). Regarding other oxidation byproducts, increased concentrations of formaldehyde, ethylene and acetaldehyde were detected. Particularly formaldehyde was formed not only in larger quantities but also at lower temperatures (43 ppm, 400 °C).

In comparison to the Fe-ZSM-5 catalyst, Cu-SSZ-13 already showed a significantly higher propylene oxidation activity at 1 bar (Figure 1a). The oxidation of C_3H_6 started at 250 °C and reached 84% conversion at 550 °C. The superior catalytic conversion of propylene was accompanied by a higher selectivity toward s CO and CO_2 formation, with a larger CO_2 fraction at low temperatures (Figure 2a and Figure S4). Analogously as observed for Fe-ZSM-5, the CO_2 proportion decreased with increasing temperature from 55% at 300 °C to 41% at 500 °C, which is in line with previous studies [26]. Although the primary oxidation products are carbon oxides, the higher conversion also resulted in increased quantities of other emissions. Thus, up to 45 ppm formaldehyde (400 °C), 5 ppm acetaldehyde (400 °C) and 18 ppm ethylene (500 °C) were measured at atmospheric pressure.

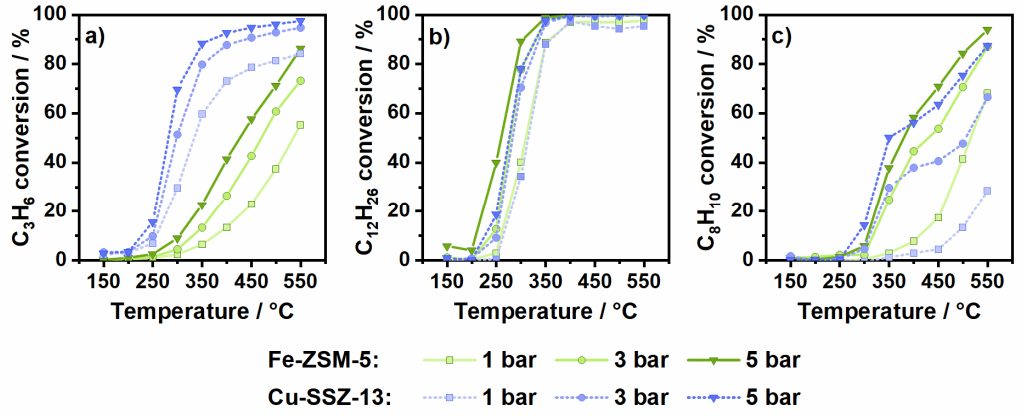

Figure 1. Hydrocarbon conversion by oxidation of (**a**) 200 ppm C_3H_6, (**b**) 50 ppm $C_{12}H_{26}$ and (**c**) 75 ppm C_8H_{10} (14% O_2, 4.5% H_2O in N_2) over Fe-ZSM-5 and Cu-SSZ-13 at 1, 3 and 5 bar pressure.

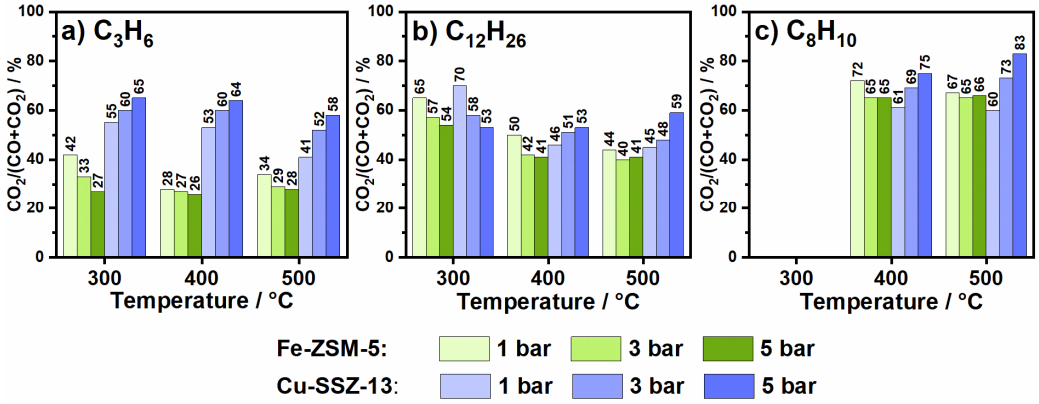

Figure 2. CO_2 proportion of formed CO_x (CO + CO_2) during hydrocarbon oxidation of (**a**) 200 ppm C_3H_6, (**b**) 50 ppm $C_{12}H_{26}$ and (**c**) 75 ppm C_8H_{10} in 14% O_2, 4.5% H_2O, N_2 over Fe-ZSM-5 and Cu-SSZ-13.

Table 1. Overview table of minor carbonaceous emissions during C_3H_6/$C_{12}H_{26}$/C_8H_{10} oxidation at 1, 3 and 5 bar pressure over Fe-ZSM-5 (Fe) and Cu-SSZ-13 (Cu).

C_3H_6 Ox.	**HCHO**			**CH_3CHO**			**C_2H_4**			**C_3H_6**		
Temperature	1 bar	3 bar	5 bar	1 bar	3 bar	5 bar	1 bar	3 bar	5 bar	1 bar	3 bar	5 bar
300 °C (Fe)	3	6	12	0	1	2	0	0	0	-	-	-
400 °C (Fe)	16	33	43	2	3	5	1	2	3	-	-	-
500 °C (Fe)	24	36	32	2	3	4	2	4	5	-	-	-
300 °C (Cu)	13	34	59	5	5	4	0	0	1	-	-	-
400 °C (Cu)	45	36	35	5	2	1	9	9	7	-	-	-
500 °C (Cu)	34	16	9	3	1	1	18	11	7	-	-	-
$C_{12}H_{26}$ Ox.	**HCHO**			**CH_3CHO**			**C_2H_4**			**C_3H_6**		
Temperature	1 bar	3 bar	5 bar	1 bar	3 bar	5 bar	1 bar	3 bar	5 bar	1 bar	3 bar	5 bar
300 °C (Fe)	6	18	32	12	26	27	1	2	2	2	2	2
400 °C (Fe)	52	70	67	16	6	2	9	8	6	5	2	1
500 °C (Fe)	28	23	14	2	0	0	11	8	5	5	1	0
300 °C (Cu)	3	7	13	6	16	23	0	1	1	0	0	0
400 °C (Cu)	25	18	15	20	11	8	7	5	3	2	1	0
500 °C (Cu)	19	4	2	12	4	2	15	4	1	3	0	0
C_8H_{10} Ox.	**HCHO**			**CH_3CHO**			**C_2H_4**			**C_3H_6**		
Temperature	1 bar	3 bar	5 bar	1 bar	3 bar	5 bar	1 bar	3 bar	5 bar	1 bar	3 bar	5 bar
300 °C (Fe)	1	1	2	0	0	1	0	0	0	0	0	2
400 °C (Fe)	3	7	9	0	3	2	0	0	0	1	18	25
500 °C (Fe)	7	11	10	2	1	0	0	0	0	0	2	2
300 °C (Cu)	0	0	1	0	1	2	0	0	0	0	0	4
400 °C (Cu)	0	1	1	1	6	4	0	0	0	1	10	17
500 °C (Cu)	0	1	1	0	4	2	0	0	0	0	6	9

Similar to the catalytic response of Fe-ZSM-5, a significant increase in propylene conversion was also achieved for Cu-SSZ-13 upon pressure increase (Figure 1a). This behavior is in agreement with that reported by Günter et al. [14] under comparable reaction conditions. The effect of pressure was particularly noticeable within the light-off temperature window, where the oxidation activity could be increased by up to 40% when changing the pressure from 1 to 5 bar. Furthermore, already at 400 °C almost complete conversion (93%) of C_3H_6 was reached at 5 bar pressure. In addition to an enhanced conversion, a larger proportion of intermediate products seem to be oxidized to CO and CO_2, with an increased percentage of CO_2 at high pressure and high temperatures (Figure 2a). Hence, the highest concentration of formaldehyde amounting to 59 ppm was observed at 300 °C and 5 bar. These emissions decrease rapidly with increasing temperature and only 9 ppm HCHO were detected at 500 °C and 5 bar pressure.

In a next step, the oxidation of *n*-dodecane was tested over the two zeolite-based catalysts. Similarly, as in the case of propylene oxidation, at 1 bar pressure Fe-ZSM-5 was able to convert *n*-dodecane above 200 °C (Figure 1b). From this temperature onwards, the activity showed a steep increase until full conversion of $C_{12}H_{26}$ was achieved at 450 °C. During *n*-dodecane oxidation, a high number of byproducts was encountered especially at low and intermediate temperatures. As shown in Figure S3, the CO_x selectivity was only 13% at 300 °C and 57% at 400 °C. In the same temperature range, the oxidation of dodecane resulted in up to 52 ppm HCHO (400 °C), 16 ppm CH_3CHO (400 °C), 9 ppm C_2H_4 (400 °C) and 11 ppm C_3H_6 (500 °C). Since with all detected byproducts the carbon balance is still not fulfilled in respect to the *n*-dodecane concentration, the formation of other compounds, which are not detected due to the limited number of FTIR calibration methods, cannot be excluded. For example, further carboxylic acids might form at low temperatures, as reported in previous oxidation studies on *n*-dodecane oxidation [22,27,28]. In contrast, at high temperatures the conversion of *n*-dodecane leads predominantly to CO

and CO_2. At these temperatures, the catalytic oxidation is probably supplemented by the gas phase conversion of *n*-dodecane that results in additional CO emissions, as previously observed for propylene [21,23,29].

The rise in pressure only had a minor effect on the oxidation of *n*-dodecane over Fe-ZSM-5 and caused a slightly earlier full conversion (Figure 1). Like for propylene oxidation, a more complete oxidation but a higher CO proportion was observed (Figure 2 and Figure S3). However, the selectivity for CO + CO_2 formation at temperatures above 400 °C was lower at 5 bar as compared to lower pressures. A possible explanation for this behavior could be the formation of additional byproducts that are favored under these conditions [30] but are not resolved by the used FTIR calibration methods. This possibility is also supported by the higher concentrations of formaldehyde (70 ppm at 400 °C and 3 bar) and acetaldehyde (27 ppm at 300 °C and 5 bar) detected at higher pressure. In contrast, shorter chain alkenes were formed less with increasing pressure.

Over Cu-SSZ-13 *n*-dodecane was fully converted at temperatures above 350 °C (Figure 1). The amount of formed CO_2 decreased with increasing temperature as also observed during propylene oxidation and for Fe-ZSM-5 (Figure 2). Thus, CO and CO_2 emissions combined only reach 55% selectivity at 500 °C (Figure S4). In comparison to the Fe-zeolite catalyst, formaldehyde formation was significantly lower (max. 25 ppm). However, slightly higher quantities of ethylene (max. 15 ppm) and acetaldehyde (max. 20 ppm) were emitted. An increase in pressure led to an earlier complete *n*-dodecane conversion for Cu-SSZ-13. Regarding reaction byproducts, the formation of formaldehyde decreases with the increase of temperature and pressure. For instance, 15 ppm HCHO were measured at 5 bar and 400 °C instead of 25 ppm as detected at the same temperature but 1 bar pressure. Likewise, the emissions of ethylene and propylene decreased with rising pressure. Only the amount of formed acetaldehyde was slightly enhanced and had a maximum value of 23 ppm at 300 °C and 5 bar. In general, a more complete oxidation was attained at high temperatures (an increase of CO_x selectivity to 90% at 500 °C and 5 bar) and an improved conversion to CO_2 (59% CO_2 share at 500 °C and 5 bar, Figure 2) due to pressure variation.

The aromatic model compound *o*-xylene (C_8H_{10}) showed the lowest conversion over the tested zeolite catalysts. Using the Fe-ZSM-5 catalyst, *o*-xylene was converted under atmospheric pressure only at temperatures above 300 °C and reached 68% conversion at 550 °C (Figure 1). Although significantly more CO_2 than CO was produced (72% CO_2 share), the CO_x selectivity at 400 °C was only 56% (Figure 2 and Figure S3). Simultaneously, only low concentrations of formaldehyde (3 ppm HCHO) and propylene (1 ppm C_3H_6) were detected at 400 °C. This likely suggests the formation of larger amounts of undetected compounds below 400 °C, such as benzaldehyde, phthalic anhydride or maleic anhydride [31–34]. As the temperature increases, the amount of carbon oxides rises significantly, leading to a CO_x selectivity of almost 90% and only 7 ppm HCHO emissions at 500 °C.

The impact of higher pressure is also clearly visible during *o*-xylene oxidation over Fe-ZSM-5, leading to an increase of conversion from 68% at 1 bar to 94% at 5 bar pressure and 550 °C. Nonetheless, the selectivity towards CO and CO_2 formation is less affected. Although the proportion of CO_2 decreases from 72% to 65% (Figure S3) when the pressure is increased from 1 to 3 bar, it does not show any further changes at higher temperatures or higher pressure. In addition, only slightly higher formaldehyde and acetaldehyde emissions were observed with increasing pressure. Only the formation of propylene seems to be promoted and 25 ppm C_3H_6 were detected at 5 bar and 400 °C. The formation of propylene during pyrolysis of *o*-xylene was reported also by Schaefgen et al. [35].

Similar to Fe-ZSM-5, the Cu-SSZ-13 catalyst shows only a low activity for the conversion of *o*-xylene, which at 1 bar pressure started above 400 °C and reached a conversion of only 14% at 500 °C (Figure 1c). The lower oxidation capacity for *o*-xylene of Cu-SSZ-13 as compared to Fe-ZSM-5 is also demonstrated by the inferior selectivity towards CO and CO_2 formation and lower concentration of CO_2 (Figure 2 and Figure S4). As shown in Table 1 almost no other byproducts were detected besides CO and CO_2. With a carbon

balance well below 100%, the formation of further byproducts is also highly probable in this case. While with increasing pressure, the amount of oxidized *o*-xylene and formed CO_2 increased, the CO_x selectivity decreased considerably. Thus, at 500 °C and 3 bar a CO_x selectivity of only 56% was measured, which is significantly lower than that recorded at 1 bar (81%). Further pressure increases to 5 bar resulted in a rise of selectivity to 69% (Figure S4). In both cases, this behavior was attributed to the formation of additional byproducts at elevated pressures.

Altogether, the results obtained at various pressures show that none of the two zeolite-based catalysts are able to completely oxidize the different model hydrocarbons used in this study. Although in some cases they fully convert the hydrocarbons with the help of high temperatures and pressure, a large number of undesirable byproducts were formed, such as CO and different aldehydes. Especially over Fe-ZSM-5 high emissions were detected whereas Cu-SSZ-13 converted the intermediates to a larger extent to CO_2. Such byproducts are expected to interfere with the SCR reactions and to lead to unwanted side reactions, as shown in the following.

2.2. Hydrocarbon Oxidation at Elevated Pressure in a Standard SCR Gas Mixture

After investigating the hydrocarbon oxidation performance of the two zeolite-based catalysts in 14% O_2, 4.5% H_2O in N_2, additional tests were conducted in a standard SCR gas mixture containing 350 ppm NO, 350 ppm NH_3, 0–200 ppm C_3H_6, 0–50 ppm $C_{12}H_{26}$, 0–75 ppm C_8H_{10}, 14% O_2 and 4.5% H_2O in N_2 balance. For Fe-ZSM-5 an increased conversion of propylene was observed at 1 bar above 250 °C in the presence of NH_3 and NO (Figure 3). Despite an enhanced oxidation of propylene, there were only small differences between the CO_x selectivity and the CO / CO_2 concentration profiles compared to the values measured in a gas mixture consisting of 14% O_2, 4.5% H_2O and N_2 (Figure 2 and Figures S3, S5 and S6). Even the amount of the other byproducts formed (formaldehyde, acetaldehyde and ethylene) did not show a major variation in concentration, suggesting a similar oxidation mechanism. The only notable difference was a sudden formation of significant amounts of hydrogen cyanide (29 ppm HCN at 500 °C, Table 2). Recent studies have shown that HCN can be formed by the reaction of NH_3 and HCHO over conventional SCR catalysts [36–38]. Since the conversion of propylene over Fe-ZSM-5 leads to a large amount of HCHO, this is most probably directly involved in HCN formation.

The increase of pressure also led to a higher propylene conversion over Fe-ZSM-5 for the standard SCR gas mixture. Nonetheless, the selectivity and byproduct concentration profiles were similar to those during the hydrocarbon oxidation tests in absence of NO and NH_3. A strong effect was observed on the HCN emissions, which were reduced down to 13 ppm at 500 °C by increasing the pressure to 5 bar.

In contrast to Fe-ZSM-5, Cu-SSZ-13 exhibited a lower oxidation performance for propylene in the SCR gas mixture, with up to 25% (350 °C, 1 bar) worse than that measured in 14% O_2, 4.5% H_2O in N_2 (Figures 1 and 3). This could be due to simultaneous reactions, which compete with hydrocarbon oxidation for active sites especially at low temperatures. Whereas less formaldehyde could be detected in the SCR gas mixture, additional emissions of HCN were measured at atmospheric pressure. Similar to Fe-ZSM-5, the enhancement of pressure resulted in a decrease of the HCN emissions (only 4 ppm at 5 bar and 400 °C) and an increase of propylene conversion (Table 2 and Figure 3). Furthermore, analogous to the absence of NO and NH_3 (Figure 2), a higher CO_x selectivity and CO_2 amount (Figure S5) were measured especially at high temperatures.

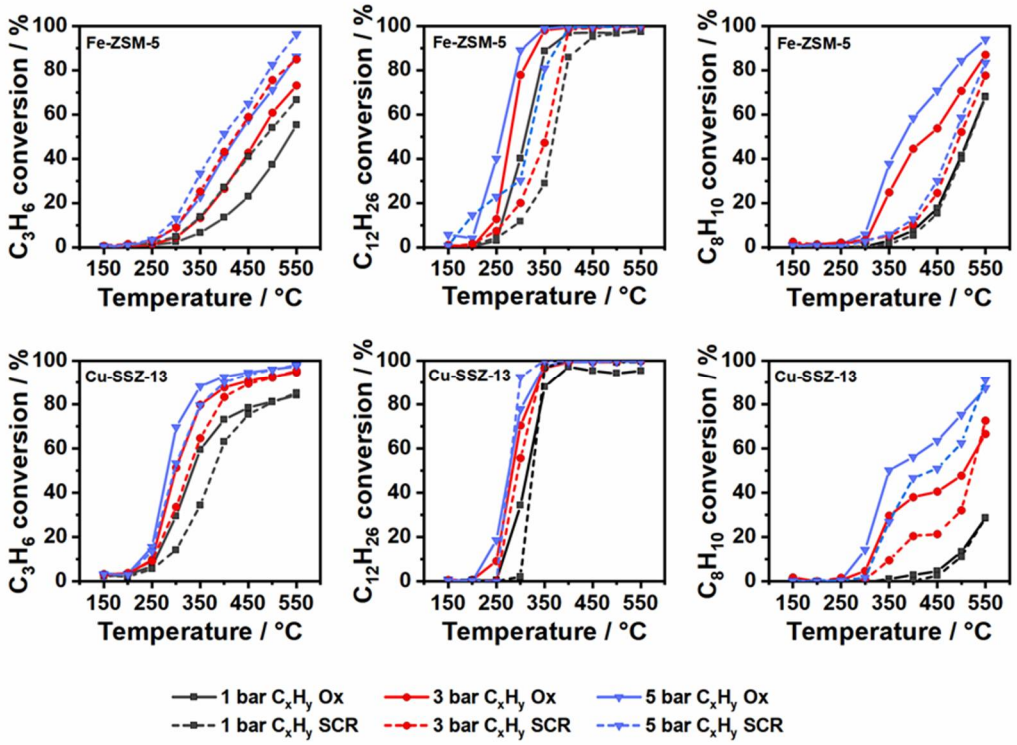

Figure 3. Hydrocarbon conversion by oxidation of 200 ppm C_3H_6 (left), 50 ppm $C_{12}H_{26}$ (middle) and 75 ppm C_8H_{10} (right) during C_xH_y oxidation (line) and standard SCR (dashed) over Fe-ZSM-5 (top) and Cu-SSZ-13 (bottom) at 1, 3 and 5 bar pressure.

Table 2. Overview table of minor carbonaceous emissions (given in ppm) during standard SCR in presence $C_3H_6/C_{12}H_{26}/C_8H_{10}$ at 1, 3 and 5 bar pressure over Fe-ZSM-5 (Fe) and Cu-SSZ-13 (Cu).

StdSCR-C_3H_6	**HCHO**			**CH_3CHO**			**C_2H_4**			**HCN**		
Temperature	1 bar	3 bar	5 bar	1 bar	3 bar	5 bar	1 bar	3 bar	5 bar	1 bar	3 bar	5 bar
300 °C (Fe)	3	7	11	1	4	3	0	0	0	2	3	4
400 °C (Fe)	19	35	44	3	3	3	1	2	2	19	19	14
500 °C (Fe)	21	26	23	2	4	3	2	3	3	29	29	13
300 °C (Cu)	2	12	28	0	2	3	0	0	1	7	10	8
400 °C (Cu)	19	28	23	5	4	1	5	7	7	28	9	4
500 °C (Cu)	23	13	8	3	0	0	16	11	6	5	0	0
StdSCR-$C_{12}H_{26}$	**HCHO**			**CH_3CHO**			**C_2H_4**			**HCN**		
Temperature	1 bar	3 bar	5 bar	1 bar	3 bar	5 bar	1 bar	3 bar	5 bar	1 bar	3 bar	5 bar
300 °C (Fe)	1	3	6	2	3	6	0	0	0	1	1	3
400 °C (Fe)	43	39	32	15	9	6	4	3	3	22	20	13
500 °C (Fe)	17	11	4	3	1	1	9	6	2	37	4	0
300 °C (Cu)	1	8	13	1	0	21	0	0	1	0	0	0
400 °C (Cu)	28	20	17	20	24	8	8	5	3	11	2	1
500 °C (Cu)	20	5	2	13	6	1	14	5	1	2	0	0
StdSCR-C_8H_{10}	**HCHO**			**CH_3CHO**			**C_3H_6**			**HCN**		
Temperature	1 bar	3 bar	5 bar	1 bar	3 bar	5 bar	1 bar	3 bar	5 bar	1 bar	3 bar	5 bar
300 °C (Fe)	0	1	1	0	0	0	0	0	0	0	0	0
400 °C (Fe)	1	3	4	0	0	0	0	0	0	1	1	1
500 °C (Fe)	4	6	7	0	0	1	0	0	0	9	5	3
300 °C (Cu)	0	0	0	0	0	0	0	0	0	0	0	0
400 °C (Cu)	0	1	2	0	3	6	0	2	9	0	0	0
500 °C (Cu)	1	2	4	0	4	6	1	2	6	0	0	0

During *n*-dodecane oxidation in the standard SCR gas mixture, a decreased conversion of *n*-dodecane was observed for both catalysts. This effect was particularly pronounced for Fe-ZSM-5, which consequently would need higher temperatures than Cu-SSZ-13 to fully convert $C_{12}H_{26}$ (Figure 3). This trend is also visible at higher pressures. In the case of Cu-SSZ-13, a small detrimental effect is noticeable at 3 and 5 bar pressure. Similar to C_3H_6 conversion, HCN emissions were observed over both catalysts. Especially for Fe-ZSM-5, large amounts of HCN (37 ppm) were detected, which further increased with rising temperature. The increase of pressure diminished the HCN formation over both catalysts, and in the case of Cu-SSZ-13 led to almost no HCN emissions at high pressure (1 ppm at 5 bar and 400 °C). A similar behavior could be observed for the other byproducts, although in the case of formaldehyde significant amounts were still emitted (Cu-SSZ-13: 17 ppm vs. Fe-ZSM-5: 32 ppm HCHO at 400 °C and 5 bar).

When comparing the *o*-xylene conversion in presence and absence of NO and NH_3, a significant drop of oxidation activity was observed for both zeolite-based catalysts at elevated pressure. The influence on Fe-ZSM-5 was more severe with a loss in *o*-xylene conversion of up to 45% (400 °C, 5 bar). Even when the pressure was increased to 5 bar, only a slight increase in *o*-xylene conversion (15–18%) was observed compared to the activity measured at 1 bar despite of the corresponding increase in residence time (Figure 3). Additionally, in case of Cu-SSZ-13, the *o*-xylene conversion for higher pressure was inhibited. This inhibition was less pronounced compared to the Fe-ZSM-5 case, and only noticeable in the temperature range from 300–500 °C. For Cu-SSZ-13 the largest decrease in the *o*-xylene oxidation activity was 23% at 350 °C and 5 bar pressure. As a result of the lower oxidation performance, also smaller concentrations of byproducts were measured for the two catalysts under these reaction conditions. Regarding the CO_x selectivity and CO_2 proportion, only minor changes were observed compared to the O_2,H_2O/N_2 gas mixture. The only pronounced difference, noticed for the two catalysts when monitoring the *o*-xylene oxidation, was a significantly lower concentration for the C_3H_6 byproduct, of max. 9 ppm at 500 °C and 5 bar in the case of Cu-SSZ-13 whereas no emissions could be detected for Fe-ZSM-5. HCN formation could only be observed in the case of the Fe-ZSM-5 catalyst and reached a maximum concentration of 9 ppm at 500 °C and 1 bar pressure.

Overall, the impact of the standard SCR gas mixture on the catalytic oxidation of the three classes of hydrocarbons used in this study showed different trends, also depending on the catalyst type. Whereas over Fe-ZSM-5 propylene oxidation was significantly promoted at all pressures in the presence of NO and NH_3, a decrease in activity was observed when using the Cu-SSZ-13 catalyst. In contrast, almost regardless of the applied pressure, the SCR gas mixture only had a moderate effect on the *n*-dodecane oxidation over the Cu-exchanged zeolite but led to a pronounced conversion decrease during the test conducted for Fe-ZSM-5. Finally, *o*-xylene oxidation is affected the most by the standard SCR gas mixture, almost irrespective of the catalyst type. In addition, the formation of byproducts was clearly influenced by the NH_3-SCR gas feed, suggesting additional reaction paths. Especially the formation of HCN over both SCR catalysts in the presence of hydrocarbons is of particular concern, as this compound is highly toxic [33]. All these variations are most probably related not only to the nature of the hydrocarbon and interaction with Cu-SSZ-13 or Fe-ZSM-5 but also to the predominantly competing SCR reactions, as it will be shown in the next section.

2.3. Impact of Elevated Pressure and Hydrocarbon Presence on NO_x Conversion

In addition to the hydrocarbon oxidation and generation of polluting carbonaceous species, the impact of hydrocarbons on the SCR of NO_x with NH_3 at elevated pressure is highly important for the pre-turbocharger application of Fe- and Cu-zeolite based catalysts. As shown in Figure 4 and also reported in recent studies [14–16], the increase of pressure has a positive effect on the catalytic NO_x removal due to the longer residence time of the reactant molecules. Since the Cu-SSZ-13 catalyst already exhibits a good activity under the applied reaction conditions, the gain in NO_x removal is less pronounced as compared

to that observed for Fe-ZSM-5. Both catalysts show the typical behavior in the absence of hydrocarbons described in literature for high pressure conditions: a superior NO_x conversion at low temperatures but rather high N_2O emissions were measured for Cu-SSZ-13 while a good catalytic activity at moderate to high temperatures but almost no N_2O emissions were obtained for the Fe-zeolite catalyst [39,40].

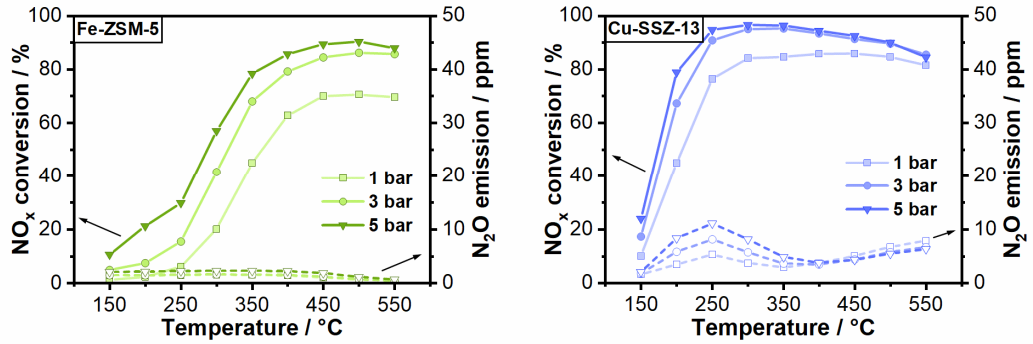

Figure 4. NO_x conversion and N_2O emission of Fe-ZSM-5 (**left**) and Cu-SSZ-13 (**right**) during standard SCR conditions (350 ppm NO, 350 NH_3, 14% O_2, 4.5% H_2O in N_2) at a GHSV of 100,000 h^{-1} and varying pressure from 1 to 5 bar.

The influence of the different hydrocarbons on the SCR activity over Fe-ZSM-5 at selected temperatures and pressures in comparison to the activity measured under typical standard SCR conditions (atmospheric pressure and absence of hydrocarbons) is depicted in Figure 5. The results show that the presence of propylene led to a slightly lower NO_x conversion at 1 bar pressure. As the temperature rises, the negative effect increases until an activity loss of 12% is reached at 500 °C. Due to its larger pores, ZSM-5 is known to be more susceptible to hydrocarbon poisoning and coking [41,42]. Another reason for the loss of activity could be the HCN formation, which involves parasitic NH_3 consumption in a reaction with HCHO [36]. However, this negative effect appears to be compensated by elevated pressures. For instance, an increase of pressure to 3 bar resulted in up to 14% higher conversion and a further increase to 5 bar in up to 33% higher conversion compared to the SCR of NO_x with NH_3 in absence of hydrocarbons.

The influence of long-chain hydrocarbons, represented in this study by $C_{12}H_{26}$, on the NH_3-SCR reaction was more severe for the Fe-ZSM-5 catalyst. At ambient pressure, *n*-dodecane presence led to a catalytic activity reduction of up to 17% (Figure 5). Even before the onset of its conversion, *n*-dodecane showed a strong inhibitory effect, most probably due to adsorption and blockage of the active sites [43]. The diffusion and significant adsorption of *n*-dodecane into the larger pores of the ZSM-5 framework could be demonstrated by a temperature programmed desorption (TPD) experiment after simultaneous adsorption of NH_3 and $C_{12}H_{26}$ at 150 °C (Figure S8). At higher temperatures, as the *n*-dodecane oxidation starts, the loss of NO_x reduction activity is even more severe. The decrease in activity is most probably due to additional competition for active sites of SCR reactants and *n*-dodecane oxidation intermediates. Like in the case of propylene, the reaction between the HCHO byproduct and NH_3 leading to HCN formation could also contribute to the diminishment of NO_x conversion. Due to the stronger negative impact of *n*-dodecane on the NH_3-SCR activity of Fe-ZSM-5 especially at temperatures below 400 °C, a pressure of 3 bar seems not sufficient to compensate for the loss of performance. However, the 5 bar pressure combined with higher temperatures counterbalances the decrease in activity. Interestingly, a further drop in NO_x conversion was encountered for the same pressure at 500 °C. The decrease might be due to the NH_3 overconsumption in reactions involving reaction byproducts, which could form on the catalyst surface or in the gas phase. This overconsumption of NH_3 is very pronounced at high pressure (Figure 6) and it is also accompanied by significant N_2O emissions (35 ppm at 550 °C and 5 bar pressure). In the study by Günter et al., [14] a similar behavior was observed in the presence of propylene, which was found to promote NO oxidation to NO_2 in the gas phase and to contribute to

the non-selective oxidation of NH_3. Since dodecane is as well converted in the gas phase at moderate temperatures already at atmospheric pressure [21,29], such reactions could lead to the formation of numerous reactive species that are ultimately involved in the drastic increase in NH_3 consumption.

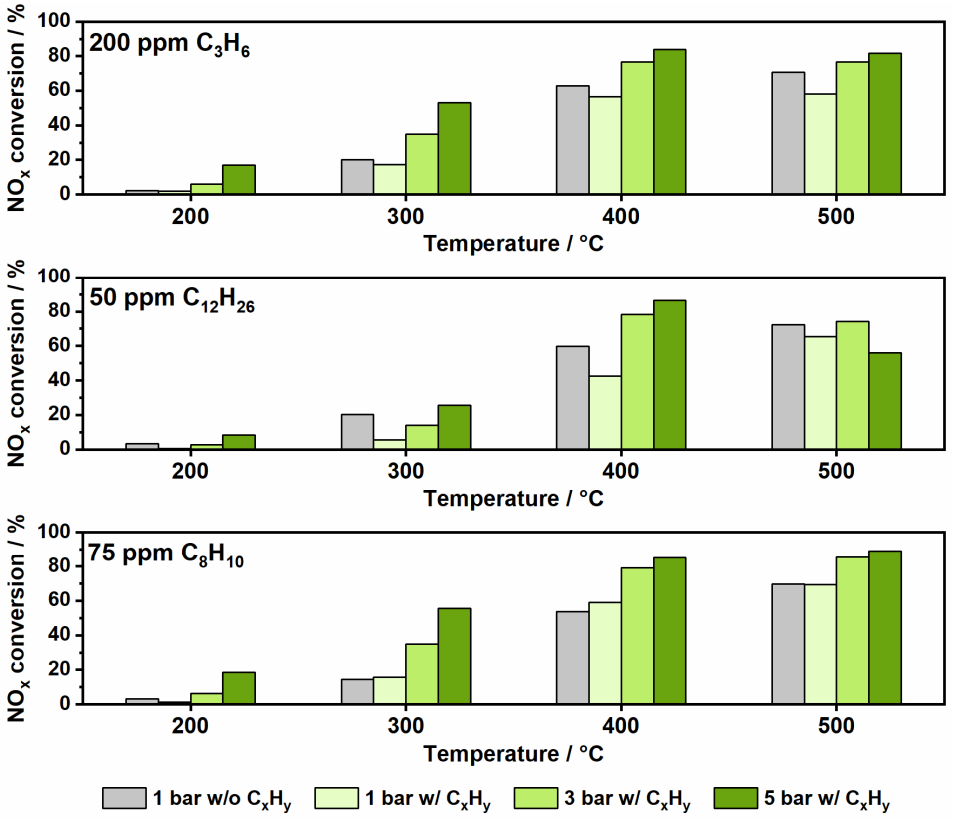

Figure 5. Comparison of NO_x conversion at conventional conditions (1 bar in absence of hydrocarbons) and under pre-turbocharger conditions (1, 3 and 5 bar in presence of hydrocarbons) over a Fe-ZSM-5 in a standard SCR gas mixture.

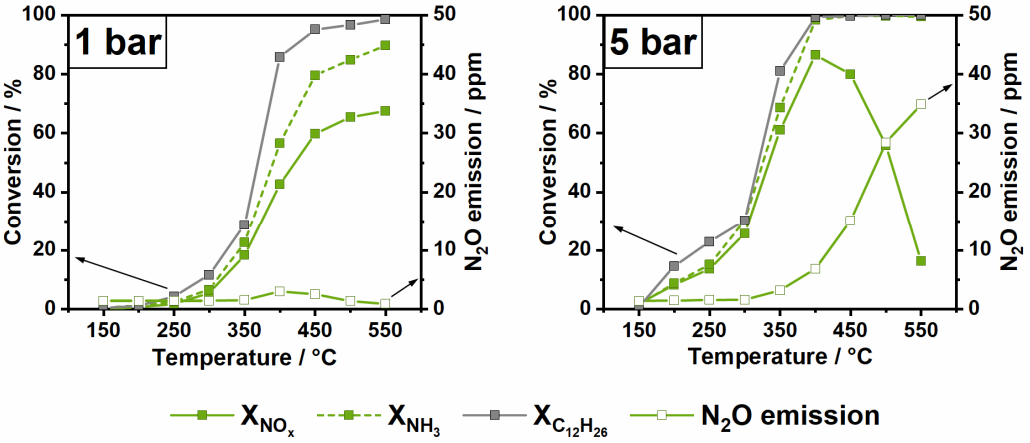

Figure 6. $NO_x/NH_3/C_{12}H_{26}$ conversion and N_2O emission over Fe-ZSM-5 for 1 bar (left) and 5 bar (right) in a standard SCR gas mixture.

In contrast to propylene and *n*-dodecane, the aromatic compound *o*-xylene has a minor impact on NO_x conversion over Fe-ZSM-5. As shown in Figure 3 and Figure S3, this is in line with the poor conversion and minimal adsorption of *o*-xylene on both zeolite-based catalysts, especially at low temperatures. Even when C_8H_{10} starts to be oxidized (above

350 °C) the influence on the NO_x conversion remains extremely low at atmospheric pressure for Fe-ZSM-5. By increasing the pressure, the NH_3-SCR activity was enhanced, and even reached the highest conversions over the entire temperature range in comparison to that obtained in the presence of the short and long-chain aliphatic hydrocarbons. Moreover, almost no differences in NO_x conversion were observed compared to the activity tests without hydrocarbons (Figure 4).

Analogous to Fe-ZSM-5, the presence of propylene interferes with the NO_x conversion on Cu-SSZ-13 (Figure 7). At 1 bar pressure the loss of activity was observed over the entire temperature range but becomes less pronounced above 400 °C (14% less NO_x conversion at 200 °C vs. 8% less NO_x conversion at 500 °C). In the literature, this deactivation by propylene has been ascribed to different effects depending on the investigated temperature range [44]. At low temperatures (150–300 °C) it is assumed that propylene blocks the catalyst surface and the opening of the pores and thus hinders the reaction of NO_x with NH_3. In the medium temperature range, when the oxidation of propylene begins, adsorption of intermediates or coking of the zeolite pores occurs. The resulting surface species are oxidized at high temperatures, leading to the recovery of the NH_3-SCR activity [44]. In addition to the blockage of the surface sites, the effect of competing reactions should be considered as well. Thus, the formation of high HCN concentrations suggests a simultaneous reaction of NH_3 with HCHO, which is a propylene oxidation byproduct [36]. The enhancement of pressure also promotes the NO_x conversion for Cu-SSZ-13 and, as expected, compensates the negative impact of C_3H_6 presence. As Cu-SSZ-13 already shows a high catalytic activity at intermediate and high temperatures, the improvement in NO_x reduction is mostly noticeable in the low temperature range. However, analogous to Fe-ZSM-5, a decrease of NH_3-SCR activity was observed at 500 °C and 5 bar pressure. This effect was also attributed to gas phase reactions of propylene and other components of the SCR gas mixture [14], leading to additional NH_3 consumption.

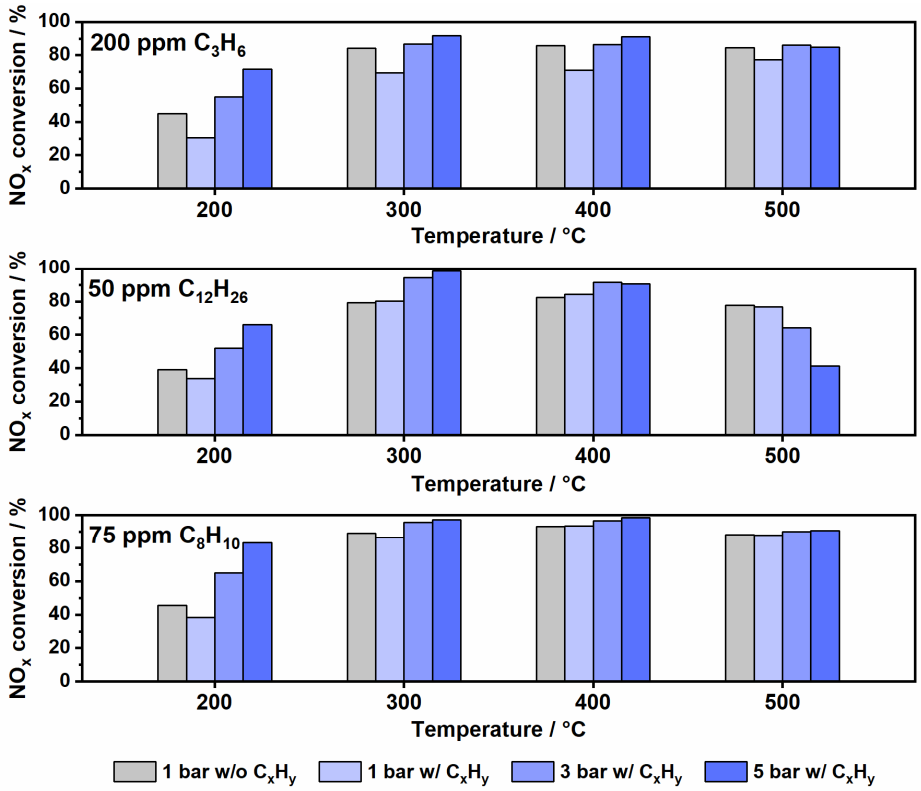

Figure 7. Comparison of NO_x conversion at conventional conditions (1 bar in absence of hydrocarbons) and under pre-turbocharger conditions (1, 3 and 5 bar in presence of hydrocarbons) over a Cu-SSZ-13 in a standard SCR gas mixture.

At atmospheric pressure, the presence of *n*-$C_{12}H_{26}$ only showed a minor effect on the NO_x reduction reaction at 200 °C. At higher temperatures, no visible influence could be observed probably due to the smaller pore size of the SSZ-13 zeolite, which prevents *n*-dodecane from entering the zeolite pore [45]. This possibility was also confirmed by an adsorption/desorption test, which showed no detectable amounts of *n*-dodecane during heating up to 550 °C after adsorption of NH_3 and $C_{12}H_{26}$ at 150 °C (Figure S8). Additionally, at higher pressures, no significant loss of activity could be observed up to 400 °C, leading to a comparable NO_x conversion to that obtained in the hydrocarbon-free gas mixture. Similar to Fe-ZSM-5, undesired gas phase reactions at 500 °C and 5 bar negatively influence the NO_x removal activity of Cu-SSZ-13 by consuming NH_3 and leading to N_2O emissions (Figure S9). Since the catalytic oxidation of NH_3 over Cu-SSZ-13 is in general more pronounced than over Fe-ZSM-5, the consumption of NH_3 is even more noticeable in this case.

Apart from a slight loss of activity at 200 °C and 1 bar pressure (7% lower NO_x conversion), in the presence of *o*-xylene no decrease of NO_x conversion was found for the other investigated temperature and pressure variations. As shown in Figure 4, for Fe-ZSM-5 the improvement of NO_x conversion obtained upon pressure increase shields any potential interference of *o*-xylene conversion on the NH_3-SCR activity (Figure 7). The gain in activity was particularly high in the low temperature range where the NO_x conversion increased by 35% at 200 °C.

The results thus show that the influence of HCs on NO_x conversion is strongly dependent on the catalyst used and the type of hydrocarbon in the gas mixture. While propylene only had a minor influence at high temperatures for the Fe-ZSM-5 catalyst, a significant inhibition was observed for Cu-SSZ-13 over the entire temperature range. However, Fe-ZMS-5 was particularly sensitive to the long-chain *n*-dodecane, which inhibited the catalytic active sites by adsorption in large amounts on the catalyst surface. No significant effects were observed for *o*-xylene with either catalyst, which could also be due to a steric limitation. By increasing the pressure, most of the observed negative effects could be compensated or diminished. However, a pronounced loss of activity was observed at high temperature and pressure if aliphatic hydrocarbons are present in the gas feed.

3. Materials and Methods

3.1. Catalyst Preparation

In this study a Fe-ZSM-5 catalyst with a Fe loading of 1.5 wt.% and a Cu-SSZ-13 catalyst with a Cu loading of 1.7 wt.% were prepared and coated on honeycombs prior to the testing procedures. Fe-ZSM-5 was synthesized by ion exchange of a commercially purchased NH_4-ZSM-5 (Si/Al = 12, MFI framework type), analogous to the study of Jablonska et al. [46]. The obtained ion exchanged zeolite was washed with deionized water and dried at 70 °C in static air. Subsequently the catalyst was calcined at 550 °C for 4 hours. For Cu-SSZ-13, an ion exchange of commercially purchased NH_4-SSZ-13 (Si/Al = 14, CHA framework type) was carried out, as described in detail in the study of Günter et al. [47]. Afterwards the sample was washed, dried and calcined similarly to Fe-ZSM-5. After preparation, both catalysts were washcoated on cordierite honeycombs (2.54 cm diameter, 3 cm length and a cell density of 400 cpsi) by dip coating. The slurry was obtained by mixing appropriate amounts of catalyst powder with 8 wt.% LUDOX AS-40 and 45 mL of deionized water. The resulting honeycombs were coated and dried several times until the desired amount of washcoat loading was achieved, and finally calcined at 550 °C for 4 h. For each hydrocarbon test series, a new honeycomb sample was prepared. The amount of washcoat for each sample is listed in Table S1.

3.2. Catalyst Characterization

Before the catalyst powders were applied to the honeycomb, they were characterized in terms of their structural and chemical properties. XRD patterns were collected for the as

prepared catalyst powders using a D8 Advanced X-ray diffractometer (Bruker AXS GmbH, Karlsruhe, Germany) with Cu Kα radiation. All diffractograms were recorded over a 2θ range of 5–50° for both zeolites. A Belsorp Mini II instrument (MicrotracBEL, Osaka, Japan) was used to determine the surface area and the pore volume of the catalysts. Prior to the analysis, approximately 80 mg of the samples were degassed at 300 °C under vacuum for 2 hours. Afterwards, adsorption and desorption of N_2 was measured and evaluated with the Belsorp Data Analysis Software using the Brunauer-Emmet-Teller (BET) isotherm. The elemental composition was identified by X-ray fluorescence (XRF) analysis at the Institute for Applied Materials (IAM-AWP, KIT, Karlsruhe, Germany). The x-ray diffractograms of the two prepared zeolites are shown in Figures S1 and S2 (supporting information). The sole presence of zeolite reflections confirms the absence of larger Cu and Fe oxides on the catalyst. The results of N_2 physisorption and elemental analysis are shown in Table 3.

Table 3. Catalyst properties determined by elemental analysis (XRF) and N_2 physisorption.

	Fe-ZSM-5	**Cu-SSZ-13**
Amount of ion exchanged metal [wt.%]	1.5	1.7
Surface area [m^2 g^{-1}]	410	770
Pore volume [mL g^{-1}]	0.2	0.3

3.3. Test Bench and Procedure

Catalytic activity and temperature programmed desorption (TPD) tests were performed in a high-pressure test bench of the Exhaust Gas Center Karlsruhe (KIT, Karlsruhe, Germany). This test bench essentially consisted of a regulated gas dosage, a countercurrent reactor and a gas analysis instrument. All gases were dosed using mass flow controllers (Bronkhorst, Leonhardsbuch, Germany). The pressure was regulated by means of a back-pressure regulator. For the analysis of the gas composition an MKS Multigas 2030 Fourier-transform infrared spectrometer (FTIR, MKS Instruments Deutschland GmbH, Munich, Germany) was used. All gas lines were heated to 175 °C before and after the catalytic reactor. The reactor, gas pipes and FTIR gas cell were entirely coated by chemical vapor deposition with a Si-based coating by SilkoTek (225 PennTech Drive, Bellefonte, PA 16823, United States), which prevents reactions catalyzed by the reactor wall. A more detailed description of the used test bench can be found in the study of Günter et al. [14]. In addition to the dosage of gaseous compounds, the dosage of liquid hydrocarbons, i.e., *n*-dodecane or *o*-xylene, was done via a heated gas saturator. By varying the temperature and the N_2 carrier flow, the concentrations of liquid hydrocarbons could be adjusted as required in the gas phase. For all catalytic tests and TPD measurements, a space velocity (GHSV) of 100,000 h^{-1} was used which corresponds to a total flow of about 25.3 L min^{-1} for the honeycomb size used in this study. For the desorption experiments, NH_3 and the hydrocarbon model compound (gas mixture: 350 ppm NH_3, 50 ppm $C_{12}H_{26}$ (C_1=600), 4.5% H_2O in N_2) were simultaneously adsorbed on the honeycomb for half an hour at 150 °C. Subsequently, after being purged in N_2 for one hour, the honeycomb was heated to 550 °C in a N_2 flow at a heating rate of 5 K min^{-1}. In the case of the catalytic activity tests, the model gas mixtures used consisted of 0/350 ppm NO, 0/350 ppm NH_3, 0/200 ppm C_3H_6, 0/50 ppm $C_{12}H_{26}$, 0/75 ppm C_8H_{10}, 4.5% H_2O, 14% O_2 and an N_2 balance depending on the experiment conditions. Each honeycomb was conditioned in reaction mixture, including the corresponding hydrocarbon, at 550 °C for 1 hour prior to the catalytic testing, so that no structural changes occur on the catalyst and only the direct influence of the hydrocarbons on the activity can be evaluated. Before each test series, the catalyst was treated at 550 °C in 14% O_2/N_2 for one hour. Then, starting at 550 °C all gas mixtures in the presence of the corresponding hydrocarbon (200 ppm C_3H_6/50 ppm $C_{12}H_{26}$/75 ppm C_8H_{10}) were tested under quasi-stationary conditions starting with standard SCR followed by hydrocarbon oxidation before the next temperature point was reduced by 50 K. This procedure was carried out down to 150 °C. After all tests were performed in the presence of

hydrocarbons, the catalyst was baked out at 550 °C in O_2/N_2 and the same measurements were performed in absence of hydrocarbons as a reference.

4. Conclusions

In this systematic study, two common zeolite-based SCR catalysts (Fe-ZSM-5 and Cu-SSZ-13) were investigated with respect to their NO_x conversion at the pre-turbocharger catalyst location, particularly considering the influence of different hydrocarbons and increased pressure. It was found that the presence of hydrocarbons in the gas mixture leads to significant catalyst deactivation and production of further harmful emissions in significant concentrations. Representative classes of hydrocarbons were used, including short-chain (C_3H_6), long-chain ($C_{12}H_{26}$) and aromatic (C_8H_{10}) hydrocarbons, during NH_3-SCR tests at various pressures and over a broad temperature range. At ambient pressure, the two tested catalysts showed only moderate activity for C_3H_6 and C_8H_{10} oxidation, and only $C_{12}H_{26}$ was almost completely converted above 400 °C. In the presence of the standard SCR gas components (NO and NH_3) the HC conversion was negatively influenced, apart from propylene oxidation over Fe-ZSM-5. In all cases, notable amounts of CO, HCHO, C_2H_4 and CH_3CHO emissions were identified alongside CO_2. Both catalysts also produced large amounts of HCN under all tested NH_3-SCR conditions involving the presence of hydrocarbons, which is due to the reaction between HCHO and NH_3 [36].

The increase of pressure resulted in enhanced hydrocarbon oxidation over both zeolite-based catalysts, mainly leading to CO and CO_2. Furthermore, lower HCN emissions were generally observed. Although the effect of higher pressure was mostly positive, it also increased harmful byproduct emissions at lower temperatures (300–400 °C). With respect to the NO_x conversion, a major boost of the NH_3-SCR activity was obtained at elevated pressures. However, the presence of hydrocarbons significantly diminished this effect especially at low temperatures. In general, the short-chained hydrocarbon showed a stronger influence on the NO_x removal activity of both zeolite-based catalysts, which was attributed to the blockage of the zeolite pores. A similar trend was observed below 300 °C if *n*-dodecane or *o*-xylene were added to the SCR gas mixture. For Fe-ZSM-5, the decrease in activity seems to be due to the *n*-dodecane adsorption and inhibition of the active sites. An additional drop in the NO_x conversion was uncovered for both catalysts above 500 °C. This effect was attributed to the overconsumption of NH_3 via parasitic reactions with *n*-dodecane oxidation intermediates or byproducts. Above 300 °C, with increasing pressure the aromatic hydrocarbon *o*-xylene showed neither a direct influence on the NO_x removal activity nor the occurrence of side reactions consuming NH_3.

Overall, if more complex gas mixtures are considered the catalyst location at the pre-turbocharger position seems to benefit especially at intermediate temperatures. Between 300 and 500 °C the increase of pressure compensates the negative effect of HC presence. A superior SCR activity could be maintained for both zeolite-based catalysts with respect to the activity measured at atmospheric pressure which demonstrates the potential of such an application for NO_x removal. Nonetheless, considering the significant emissions of HCN, formaldehyde, CO and further observed byproducts, either the improvement of the SCR catalysts or the presence of a downstream DOC seems to be mandatory for their removal.

Supplementary Materials: The following data is available online at https://www.mdpi.com/2073-4344/11/3/336/s1, Figure S1: XRD patterns of NH_4-ZSM-5 (before ion exchange) and Fe-ZSM-5 (after ion exchange), Figure S2: XRD patterns of NH_4-SSZ-13 (before ion exchange) and Cu-SSZ-13 (after ion exchange), Figure S3: CO_x selectivity (CO + CO_2) during C_xH_y oxidation (14% O_2 and 4.5% H_2O in N_2) over Fe-ZSM-5 at 1,3 and 5 bar pressure, Figure S4: CO_x selectivity (CO + CO_2) during C_xH_y oxidation (14% O_2 and 4.5% H_2O in N_2) over Cu-SSZ-13 at 1, 3 and 5 bar pressure, Figure S5: CO_2 share of formed CO_x (CO + CO_2) via hydrocarbon oxidation during standard SCR over Fe-ZSM-5 and Cu-SSZ-13, Figure S6: CO_x selectivity (CO + CO_2) during C_xH_y oxidation in standard SCR gas mixture (350 ppm NO, 350 ppm NH_3, 14% O_2 and 4.5% H_2O in N_2) over Fe-ZSM-5 at 1,3 and 5 bar pressure, Figure S7: CO_x selectivity (CO + CO_2) during C_xH_y oxidation in standard SCR gas mixture (350 ppm NO, 350 ppm NH_3, 14% O_2 and 4.5% H_2O in N_2) over Cu-SSZ-13 at 1,3 and 5 bar pressure,

Figure S8: $NO_x/NH_3/C_{12}H_{26}$ conversion and N_2O emission over Fe-ZSM-5 for 1 bar (left) and 5 bar (right) in Standard SCR gas mixture (50 ppm $C_{12}H_{26}$, 350 ppm NO, 350 ppm NH_3, 14% O_2, 4.5% H_2O in N_2), Table S1: Washcoat loading of Fe-ZSM-5 and Cu-SSZ-13 honeycombs.

Author Contributions: Conceptualization and Methodology, D.Z., M.C. and J.-D.G.; Investigation, D.Z., M.C., J.-D.G., S.B.; Experiments, D.Z. and S.B.; Writing-original draft preparation, D.Z. and M.C.; Writing—review and editing, S.B., M.C., J.-D.G.; Supervision, M.C. and J.-D.G. All authors have read and agreed to the published version of the manuscript.

Funding: This research received funding by KIT and D. Zengel received financial support by DBU.

Data Availability Statement: All data can be obtained from the corresponding author upon reasonable request.

Acknowledgments: We thank Thomas Bergfeldt (IAM-AWP, KIT) for elemental analysis and Angela Deutsch (ITCP, KIT) for BET surface analysis of the used samples. D. Zengel gratefully thanks the Deutsche Bundesstiftung Umwelt (DBU) for financial support. We acknowledge J. Pesek for his help while operating the test bench.

Conflicts of Interest: The authors declare no conflict of interest.

References

1. Group, C. Worldwide Emission Standards and Related Regulations: Passenger Cars/Light and Medium Duty Vehicles. Available online: https://www.continental-automotive.com/getattachment/8f2dedad-b510-4672-a005-3156f77d1f85/EMISSIONBOOKLET_2019.pdf (accessed on 28 September 2020).
2. Kampa, M.; Castanas, E. Human health effects of air pollution. *Environ. Pollut.* **2008**, *151*, 362–367. [CrossRef]
3. Rani, B.; Singh, U.; Chuhan, A.K.; Sharma, D.; Maheshwari, R. Photochemical Smog Pollution and Its Mitigation Measures. *J. Adv. Sci. Res.* **2011**, *2*, 28–33.
4. Peel, J.L.; Haeuber, R.; Garcia, V.; Russell, A.G.; Neas, L. Impact of nitrogen and climate change interactions on ambient air pollution and human health. *Biogeochemistry* **2013**, *114*, 121–134. [CrossRef]
5. Likens, G.E.; Wright, R.F.; Galloway, J.N.; Butler, T.J. Acid Rain. *Sci. Am.* **1979**, *241*, 43–51. [CrossRef]
6. Maiboom, A.; Tauzia, X.; Hétet, J.-F. Experimental study of various effects of exhaust gas recirculation (EGR) on combustion and emissions of an automotive direct injection diesel engine. *Energy* **2008**, *33*, 22–34. [CrossRef]
7. Mendez, S.; Thirouard, B. Using Multiple Injection Strategies in Diesel Combustion: Potential to Improve Emissions, Noise and Fuel Economy Trade-Off in Low-CR Engines. *SAE Int. J. Fuels Lubr.* **2008**, *1*, 662–674. [CrossRef]
8. Nova, I.; Tronconi, E. *Urea-SCR Technology for deNO$_x$ after Treatment Of Diesel Exhausts*; Springer: Berlin/Heidelberg, Germany, 2014; Volume 5.
9. Guan, B.; Zhan, R.; Lin, H.; Huang, Z. Review of state of the art technologies of selective catalytic reduction of NO_x from diesel engine exhaust. *Appl. Therm. Eng.* **2014**, *66*, 395–414. [CrossRef]
10. Shan, W.; Song, H. Catalysts for the selective catalytic reduction of NO_x with NH_3 at low temperature. *Catal. Sci. Technol.* **2015**, *5*, 4280–4288. [CrossRef]
11. Yadav, D.; Prasad, R. Low Temperature de-NO_x Technology-a Challenge for Vehicular Exhaust and its Remedation: An Overview. *Procedia Technol.* **2016**, *24*, 639–644. [CrossRef]
12. Zammit, M.; DiMaggio, C.L.; Kim, C.H.; Lambert, C.; Muntean, G.G.; Peden, C.H.; Parks, J.E.; Howden, K. Future *Automotive Aftertreatment Solutions*: The 150 °C *Challenge Workshop* Report. *U.S. Drive Report* **2013**. [CrossRef]
13. Presti, M.; Scheeder, A.; Brück, R. Motornahe Abgasnachbehandlung im Nutzfahrzeug: Eine Lösung für CARB 2020 NO_x? Continental Emitec GmbH—8th Emission Control Dresden. 2016. Available online: http://wordpress.emission-control-dresden.de/8-emission-control-2016/ (accessed on 6 March 2021).
14. Günter, T.; Pesek, J.; Schäfer, K.; Bertótiné Abai, A.; Casapu, M.; Deutschmann, O.; Grunwaldt, J.-D. Cu-SSZ-13 as pre-turbine NO_x-removal-catalyst: Impact of pressure and catalyst poisons. *Appl. Catal. B Environ.* **2016**, *198*, 548–557. [CrossRef]
15. Rammelt, T.; Torkashvand, B.; Hauck, C.; Böhm, J.; Gläser, R.; Deutschmann, O. Nitric Oxide Reduction of Heavy-Duty Diesel Off-Gas by NH_3-SCR in Front of the Turbocharger. *Emiss. Control Sci. Technol.* **2017**, *3*, 275–288. [CrossRef]
16. Kröcher, O.; Elsener, M.; Bothien, M.-R.; Dölling, W. SCR vor Turbolader—Einfluss des Drucks auf die NO_x-Reduktion. *MTZ—Mot. Z.* **2014**, *75*, 68–73. [CrossRef]
17. Christensen, S.R.; Hansen, B.B.; Pedersen, K.H.; Thøgersen, J.R.; Jensen, A.D. Selective Catalytic Reduction of NO_x over V_2O_5-WO_3-TiO_2 SCR Catalysts—A Study at Elevated Pressure for Maritime Pre-turbine SCR Configuration. *Emiss. Control Sci. Technol.* **2019**, *5*, 263–278. [CrossRef]
18. Jayat, F.; Pace, L.; Konieczny, R. Vorturboladerkatalysatoren_-_Anforderungen aus aufladetechnischer Sicht sowie zukünftiger, innovativer Abgasnachbehandlungskonzepte, Emitec GmbH. 2017. Available online: https://docplayer.org/33955352-Vorturboladerkatalysatoren-anforderungen-aus-aufladetechnischer-sicht-sowie-zukuenftiger-innovativer-abgasnachbehandlungskonzepte.html (accessed on 6 March 2021).

19. Serrano, J.R.; Guardiola, C.; Piqueras, P.; Angiolini, E. *Analysis of the Aftertreatment Sizing for Pre-Turbo DPF and DOC Exhaust Line Configurations*; 2014-01-1498; SAE Technical Paper: Warrendale, PA, USA, 2014. [CrossRef]
20. Subramaniam, M.N.; Hayes, C.; Tomazic, D.; Downey, M.; Bruestle, C. Pre-Turbo Aftertreatment Position for Large Bore Diesel Engines—Compact & Cost-Effective Aftertreatment with a Fuel Consumption Advantage. *SAE Int. J. Eng.* **2011**, *4*, 106–116. [CrossRef]
21. Liu, C.-H.; Giewont, K.; Toops, T.J.; Walker, E.A.; Horvatits, C.; Kyriakidou, E.A. Non-catalytic gas phase NO oxidation in the presence of decane. *Fuel* **2021**, *286*, 119388. [CrossRef]
22. Hazlett, M.J.; Epling, W.S. Coupled Heterogeneous and Homogeneous Hydrocarbon Oxidation Reactions in Model Diesel Oxidation Catalysts. *Emiss. Control Sci. Technol.* **2017**, *3*, 5–17. [CrossRef]
23. Zengel, D.; Stehle, M.; Deutschmann, O.; Casapu, M.; Grunwaldt, J.-D. Impact of gas phase reactions and catalyst poisons on the NH_3-SCR activity of a V_2O_5-WO_3/TiO_2 catalyst at pre-turbine position. *Appl. Catal. B Environ.* **2021**, 119991. [CrossRef]
24. Starokon, E.; Vedyagin, A.; Pirutko, L.; Mishakov, I. Oxidation of CO and hydrocarbons with molecular oxygen over Fe–ZSM-5 zeolite. *J. Porous Mater.* **2015**, *22*, 521–527. [CrossRef]
25. Torkashvand, B.; Gremminger, A.; Valchera, S.; Casapu, M.; Grunwaldt, J.-D.; Deutschmann, O. *The Impact of Pre-Turbine Catalyst Placement on Methane Oxidation in Lean-Burn Gas Engines: An Experimental and Numerical Study*; 2017-01-1019; SAE Technical Paper: Warrendale, PA, USA, 2017. [CrossRef]
26. Zheng, Y.; Harold, M.P.; Luss, D. Effects of CO, H_2 and C_3H_6 on Cu-SSZ-13 catalyzed NH_3-SCR. *Catal. Today* **2016**, *264*, 44–54. [CrossRef]
27. Vakhrushin, P.A.; Vishnetskaya, M.V.; Kokorin, A.I. The oxidation of dodecane on a vanadium-molybdenum catalyst. *Russ. J. Phys. Chem. B* **2012**, *6*, 169–172. [CrossRef]
28. Vishnetskaya, M.V.; Vakhrushin, P.A. Oxidation of dodecane on transition metal oxides. *Russ. J. Phys. Chem. A* **2012**, *86*, 1664–1668. [CrossRef]
29. Luo, J.-Y.; Yezerets, A.; Henry, C.; Hess, H.; Kamasamudram, K.; Chen, H.-Y.; Epling, W.S. *Hydrocarbon Poisoning of Cu-Zeolite SCR Catalysts*; 2012-01-1096; SAE Technical Paper: Warrendale, PA, USA, 2012. [CrossRef]
30. Kurman, M.S.; Natelson, R.H.; Cernansky, N.P.; Miller, D.L. Speciation of the reaction intermediates from *n*-dodecane oxidation in the low temperature regime. *Proc. Combust. Inst.* **2011**, *33*, 159–166. [CrossRef]
31. Becker, L.; Förster, H. Investigations of coke deposits formed during deep oxidation of benzene over Pd and Cu exchanged Y-type zeolites. *Appl. Catal. A Gen.* **1997**, *153*, 31–41. [CrossRef]
32. Saleh, R.Y.; Wachs, I.E. Reaction network and kinetics of o-xylene oxidation to phthalic anhydride over V_2O_5/TiO_2 (anatase) catalysts. *Appl. Catal.* **1987**, *31*, 87–98. [CrossRef]
33. Andersson, S.L.T. Reaction networks in the catalytic vapor-phase oxidation of toluene and xylenes. *J. Catal.* **1986**, *98*, 138–149. [CrossRef]
34. Wachs, I.E.; Saleh, R.Y.; Chan, S.S.; Chersich, C.C. The interaction of vanadium pentoxide with titania (anatase): Part I. Effect on o-xylene oxidation to phthalic anhydride. *Appl. Catal.* **1985**, *15*, 339–352. [CrossRef]
35. Schaefgen, J.R. The pyrolysis of p-xylene. *J. Polym. Sci.* **1955**, *15*, 203–219. [CrossRef]
36. Zengel, D.; Koch, P.; Torkashvand, B.; Grunwaldt, J.-D.; Casapu, M.; Deutschmann, O. Emission of Toxic HCN During NO_x Removal by Ammonia SCR in the Exhaust of Lean-Burn Natural Gas Engines. *Angew. Chem. Int. Ed.* **2020**, *59*, 14423–14428. [CrossRef] [PubMed]
37. Ngo, A.B.; Vuong, T.H.; Atia, H.; Bentrup, U.; Kondratenko, V.A.; Kondratenko, E.V.; Rabeah, J.; Ambruster, U.; Brückner, A. Effect of Formaldehyde in Selective Catalytic Reduction of NO x by Ammonia (NH_3-SCR) on a Commercial V_2O_5-WO_3/TiO_2 Catalyst under Model Conditions. *Environ. Sci. Technol.* **2020**, *54*, 11753–11761. [CrossRef]
38. Elsener, M.; Nuguid, R.J.G.; Kröcher, O.; Ferri, D. HCN production from formaldehyde during the selective catalytic reduction of NO_x with NH_3 over V_2O_5/WO_3-TiO_2. *Appl. Catal. B Environ.* **2021**, *281*, 119462. [CrossRef]
39. Shi, X.; Liu, F.; Xie, L.; Shan, W.; He, H. NH_3-SCR Performance of Fresh and Hydrothermally Aged Fe-ZSM-5 in Standard and Fast Selective Catalytic Reduction Reactions. *Environ. Sci. Technol.* **2013**, *47*, 3293–3298. [CrossRef]
40. Kröcher, O.; Devadas, M.; Elsener, M.; Wokaun, A.; Söger, N.; Pfeifer, M.; Demel, Y.; Mussmann, L. Investigation of the selective catalytic reduction of NO by NH_3 on Fe-ZSM5 monolith catalysts. *Appl. Catal. B Environ.* **2006**, *66*, 208–216. [CrossRef]
41. Li, J.; Zhu, R.; Cheng, Y.; Lambert, C.K.; Yang, R.T. Mechanism of Propene Poisoning on Fe-ZSM-5 for Selective Catalytic Reduction of NO_x with Ammonia. *Environ. Sci. Technol.* **2010**, *44*, 1799–1805. [CrossRef] [PubMed]
42. Ma, L.; Li, J.; Cheng, Y.; Lambert, C.K.; Fu, L. Propene Poisoning on Three Typical Fe-zeolites for SCR of NO_x with NH_3: From Mechanism Study to Coating Modified Architecture. *Environ. Sci. Technol.* **2012**, *46*, 1747–1754. [CrossRef]
43. Heo, I.; Sung, S.; Park, M.B.; Chang, T.S.; Kim, Y.J.; Cho, B.K.; Hong, S.B.; Choung, J.W.; Nam, I.-S. Effect of Hydrocarbon on $DeNO_x$ Performance of Selective Catalytic Reduction by a Combined Reductant over Cu-Containing Zeolite Catalysts. *ACS Catal.* **2019**, *9*, 9800–9812. [CrossRef]
44. Ma, L.; Su, W.; Li, Z.; Li, J.; Fu, L.; Hao, J. Mechanism of propene poisoning on Cu-SSZ-13 catalysts for SCR of NO_x with NH_3. *Catal. Today* **2015**, *245*, 16–21. [CrossRef]
45. Ye, Q.; Wang, L.; Yang, R.T. Activity, propene poisoning resistance and hydrothermal stability of copper exchanged chabazite-like zeolite catalysts for SCR of NO with ammonia in comparison to Cu/ZSM-5. *Appl. Catal. A Gen.* **2012**, *427–428*, 24–34. [CrossRef]

46. Jabłońska, M.; Delahay, G.; Kruczała, K.; Błachowski, A.; Tarach, K.A.; Brylewska, K.; Petitto, C.; Góra-Marek, K. Standard and Fast Selective Catalytic Reduction of NO with NH_3 on Zeolites Fe-BEA. *J. Physical Chem. C* **2016**, *120*, 16831–16842. [CrossRef]
47. Günter, T.; Carvalho, H.W.; Doronkin, D.E.; Sheppard, T.; Glatzel, P.; Atkins, A.J.; Rudolph, J.; Jacob, C.R.; Casapu, M.; Grunwaldt, J.D. Structural snapshots of the SCR reaction mechanism on Cu-SSZ-13. *Chem. Commun. (Camb)* **2015**, *51*, 9227–9230. [CrossRef]